Reflection Shifts in Gold Nanoparticles

Maryam Zoghi[*,1]

[1] School of Engineering Science, College of Engineering, University of
Tehran, Enqelab Street, Tehran, Iran

Abstract: Metal nanoparticles are widely researched for the fabrication of novel low cost and more energy efficient optoelectronic devices. Optical properties of metal nanoparticles are known to be different from their bulk counterparts. In this paper, with an appropriate modification of Drude model, I provide an improved dielectric function for gold nanoparticles which accounts for particle size as well as temperature effects. The model is consequently used to investigate Goos-Hanchen and Imbert-Fedorov reflection shifts of an oblique linearly polarized laser beam reflected from the nanoparticles in various temperatures. It is shown that the beam light can contribute both spatial and angular shifts depending on its state of polarity. The maximum shifts take place at grazing angles when the polarization of light is set at TM and 45°. Study of the light deviations' sensitivity to the temperature indicates that reflection shifts decrease linearly at higher temperatures except in angular out-of-plane shift Θ_{IF}. The trend is incremental for different nanoparticle size, keeping the distinct behavior of Θ_{IF}. Such results allow more accurate prediction of many optical phenomena involving nanoscaled gold and may serve as a delicate method to determine nanoparticles' size.

1. INTRODUCTION

Noble metal nanoparticles (MNPs) attract great interest because of unique properties arising from their ability to resonate with light. Resonant excitation of localized surface plasmons on nanoparticles gives rise to a variety of effects which enable applying them as nanosensing modalities [1, 2], for photothermal cancer therapy [3], or in solar cells [4]. They are also used for surface enhanced Raman scattering, colorimetry, high-resolution microscopy, non-diffraction limited nanoscopic waveguides.

---

* Corresponding author. E-mail: **maryam.zoghi@ut.ac.ir**

Recently, the easy manipulation of colloidal MNPs has allowed their self-assembly into complex structures, 2D or 3D networks that show collective properties [5]. Networks based on MNPs have electronic and optoelectronic properties that is served in nanophotonic devices [6]. Meanwhile, the application of the thermo-optic effects as a thermodynamic means for operating optical devices, such as switch [7], attenuator [8] and filter, is currently of great concern.

It has been shown that a self-assembled monolayer of metal nanoparticles has a high reflectivity [5,6,9,10]. Of the properties of a reflective surface is the reflection shifts occur when the light bounces the interface, known as Goos-Hanchen (GH) and Imbert-Fedorov (IF) shifts. This effect has resulted in extensive field of research including weak measurement of shifts [11], GH shift in: non-absorbing [12], weakly absorbing [13], grounded slab [14], graphene coated [15] and even metasurfaces [16]. Beam shifts have also received much attention because of their potential applications in the design of optical devices such as optical waveguide switch [17] as well as optical sensors [18].

Most of the prior papers have studied the reflection shifts of bulk metals but the number of studies on self-assembled metal nanoparticles is few to my knowledge. The purpose of this work is to investigate the reflection shifts of such 2D-nanostructures. In this paper, an improved Drude-Summerfield model is used to account for GH and IF shifts response of a monolayer consisting of close-packed spherical gold NPs. The analysis examines the effect for reflection of αᵒ-linearly polarized beam at various radiation angles, particle sizes and temperatures. Control over these parameters renders such nanostructures promising media for development of novel nanodevices and optical elements.

2. THEORETICAL MODEL
A. Reflection Shifts

Nowadays, it is known that reflected beams undergo a rather universal phenomenon due to the wave nature of light. In fact, diffractive corrections displace the beam in directions parallel and perpendicular to plane of incidence [19]. The longitudinal shift is called Goos-Hanchen (GH) shift [20], while the transverse one is referred to Imbert-Fedorov (IF) shift also known as Spin Hall Effect of light [21-23]. The GH effect, priority observed in total internal reflection, originates from the dispersion of the reflection or transmission coefficient. On the other hand, IF effect is assumed to be a result of spin angular momentum carried by a polarized beam and conservation of the total angular momentum in the system as well [24]. Figure.1 indicates GH and IF shifts including spatial (Δ) and angular (Θ) parts.
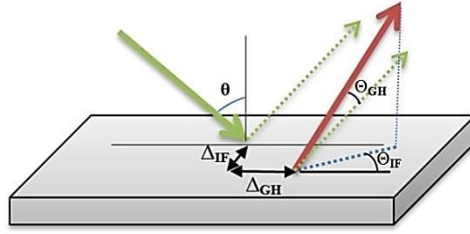
Fig.1 GH and IF shifts in a plane reflecting interface

Metals distinguish from dielectrics by their complex refractive index $\hat{n} = n + i\kappa$ where κ is the extinction coefficient. When light at the angle θ incidents from air onto a metallic surface, the complex reflection coefficients $r_m = R_m e^{i\varphi_m}$ are described with the magnitude R_m and the phase shifts φ_m defined as [19]

$$\varphi_s = Im\left(Ln\left[\frac{\cos\theta - \sqrt{\hat{n}^2 - \sin^2\theta}}{\cos\theta + \sqrt{\hat{n}^2 - \sin^2\theta}}\right]\right) \tag{1a}$$

$$\varphi_p = Im\left(Ln\left[\frac{\hat{n}^2\cos\theta - \sqrt{\hat{n}^2 - \sin^2\theta}}{\hat{n}^2\cos\theta + \sqrt{\hat{n}^2 - \sin^2\theta}}\right]\right) \tag{1b}$$

pertaining to TE(s-wave) and TM(p-wave) polarizations respectively ($m \in \{s, p\}$). The explicit expression of the GH and IF shifts for a fundamental Gaussian beam are known to be [25]

$$\Delta_{GH} = \omega_p \frac{\partial\varphi_p}{\partial\theta} + \omega_s \frac{\partial\varphi_s}{\partial\theta} \tag{2a}$$

$$-\Theta_{GH} = \omega_p \frac{\partial LnR_p}{\partial\theta} + \omega_s \frac{\partial LnR_s}{\partial\theta} \tag{2b}$$

$$\Delta_{IF} = -\cot\theta\left[\frac{\omega_p a_s^2 + \omega_s a_p^2}{a_s a_p}\sin\eta + 2\sqrt{\omega_p\omega_s}\sin(\eta - \varphi_p + \varphi_s)\right] \tag{2c}$$

$$\Theta_{IF} = \frac{\omega_p a_s^2 - \omega_s a_p^2}{a_s a_p}\cos\theta\cos\eta \tag{2d}$$

where $\omega_m = \frac{a_m^2 R_m^2}{a_s^2 R_s^2 + a_p^2 R_p^2}$ and a_m are the electric field components for parallel and perpendicular directions. The phase shift between these two components is given by η. Considering a Gaussian α°-linearly polarized beam with in-phase electric field as $E = E_0 \begin{bmatrix} \cos\alpha \\ \sin\alpha \end{bmatrix}$, the beam shifts are calculated based on equations (2). This would finally yield the total experimental shift L with measurable units consisting of spatial shift Δ in length dimension and angular shift $\frac{\Theta}{\Lambda}$ in radian dimension:

$$L = \Delta + z\frac{\Theta}{\Lambda} \tag{3}$$

Here, $\Lambda = \frac{2}{\theta_0{}^2}$, θ_0 is the opening angle of the incoming beam and Z is the distance of the detector from the beam waist. A schematic of gold nanoparticle array, Gaussian beam of laser and conceptual measurement setup are shown in Fig.2.
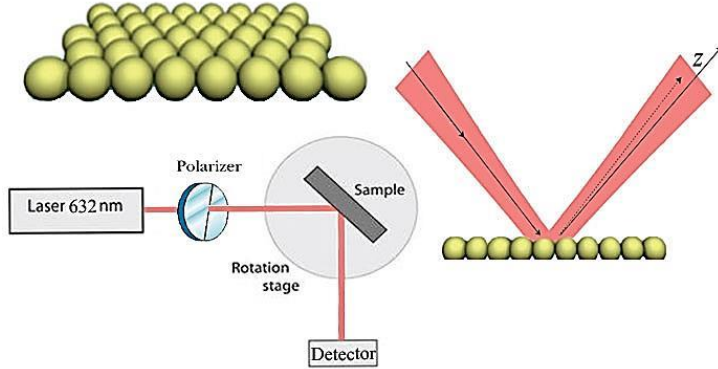

Fig.2. A schematic of close-packed gold nanoparticle array, Gaussian beam and the measurement setup.

As the reflection shifts are described by complex refractive index $\hat{n} = \sqrt{\varepsilon}$, the next step is to find dielectric function ε of metal nanoparticles.

B. Temperature-dependent Drude Model for Nanoparticles

Often used dielectric function of bulk metals results from the *fundamental* Drude model supplemented by electron relaxation:

$$\varepsilon_D(\omega) = 1 - \frac{\omega_p{}^2}{\omega^2 + i\,\omega\gamma_{bulk}} \qquad (4)$$

where ω_p is the bulk plasma frequency accounting for the number density of free electrons. The electron relaxation rate γ_{bulk} is proportional to the reciprocal of the mean free time between electron collisions in the metal.

On the other hand, when dealing with metal nanoparticles, it must be noted that they absorb and scatter light with extraordinary efficiency. Their strong interaction with light occurs because the conduction electrons on the metal surface undergo a collective oscillation when they are excited by light at specific wavelengths known as a surface plasmon (SP) resonance. The relevant frequency dependence of the nanoparticles' refractive index could be described by the *improved* Drude formula [26]:

$$\varepsilon_{imp}(\omega) = 1 - \frac{\omega_{sp}{}^2}{\omega^2 + i\,\omega\gamma} \qquad (5)$$

Here, ω_{sp} is the surface plasmon frequency that when air is the host medium is considered as [27]:

$$\omega_{sp} = \sqrt{\frac{\omega_p{}^2}{2} - \gamma^2} \tag{6}$$

The damping frequency γ of NP structure includes bulk frequency, phonon-electron scattering, electron-electron scattering and a scattering term due to particle size respectively:

$$\gamma = \gamma_{\text{bulk}} + \gamma_{ph-e} + \gamma_{e-e} + \frac{AV_F}{r} \tag{7}$$

Where A is a model-dependent constant whose values have been theoretically justified from 0.1 to 2 [28] and V_F is the Fermi velocity.

The temperature dependence of the bulk plasmon frequency is as follows:

$$\omega_p(T) = \sqrt{\frac{N(T)e^2}{m^*\epsilon_0}} \tag{8}$$

Density of electrons varies with temperature as $N(T) = \sqrt{\frac{N(T_0)}{1+\beta(T-T_0)}}$. The reference temperature T_0 is taken to be room temperature (300K) and β is the volume thermal expansion coefficient of metal. Neglecting the small variations of the effective mass of electron, m^* is considered to be constant. These terms depend on temperature as [27]:

$$\gamma_{ph-e}(T) = \frac{\omega_p{}^2}{\sigma(0)} \frac{\left[\frac{1}{10} + \left(\frac{T}{T_\theta}\right)^5 \int_0^{\frac{T_\theta}{T}} \frac{y^4}{e^y - 1} dy\right]}{\int_0^1 \frac{y^5}{(e^y - 1)(1 - e^{-y})} dy} \tag{9-a}$$

$$\gamma_{e-e}(T) = \frac{\pi^3 \Gamma \delta}{12\hbar E_f} \left[(k_B T)^2 + \left(\frac{\hbar\omega}{2\pi}\right)^2\right] \tag{9-b}$$

$$\gamma_{\text{bulk}} = \acute{K} T^5 \int_0^{\frac{T_\theta}{T}} \frac{y^4}{e^y - 1} dy \tag{9-c}$$

$$r(T) = r(T_0)[1 + \beta(T - T_0)]^{\frac{1}{3}} \tag{9-d}$$

Here, $\sigma(0)$ is the DC conductivity at $T = T_\theta$ where T_θ is Debye temperature. Γ is a constant giving the average over the Fermi surface of the scattering probability, δ represents the fractional umklapp scattering, E_f is the Fermi Energy, $\hbar$ is Plank constant and k_B is the Boltzmann constant. C and $\acute{K}$ are constants and r is the particle's radius. All the parameters used in this work are summarized in Table I.

TABLE I

VALUES OF PARAMETERS FOR GOLD

Parameter	Name	Value
$N(T_0)$	Free electron density at room temperature	$5.90 \times 10^{28} \mathrm{m}^{-3}$
m^*	Effective mass of electron	$1.1 \times \mathrm{m_e}$
$\sigma(0)$	DC conductivity at Deby temperature	$1.32 \times 10^{-8} \Omega m$
T_θ	Deby temperature	170 K
Γ	average over the Fermi surface	0.55
δ	fractional umklapp scattering	0.77
E_F	Fermi Energy	5.51ev
V_F	Fermi velocity	$1.4 \times 10^6 \, ms^{-1}$
$\acute{K}$	bulk damping rate parameter	$3.2 \times 10^{-23} HzK^{-5}$
β	volume thermal expansion coefficient	$14.2 \times 10^{-6} K^{-1}$
A	Surface scattering parameter	2

3. RESULTS AND DISCUSSION

Having determined the dielectric function of gold nanoparticles, we turn our attention to the reflection shifts. Some calculations using Mathematica were performed to investigate the reflection shifts based on eqs. (2). In Fig.3, calculated GH and IF shifts versus angle of incidence are shown for both of fundamental and improved Drude model. The behaviors of angular deviations are similar to their spatial partners depicted on the right axis.
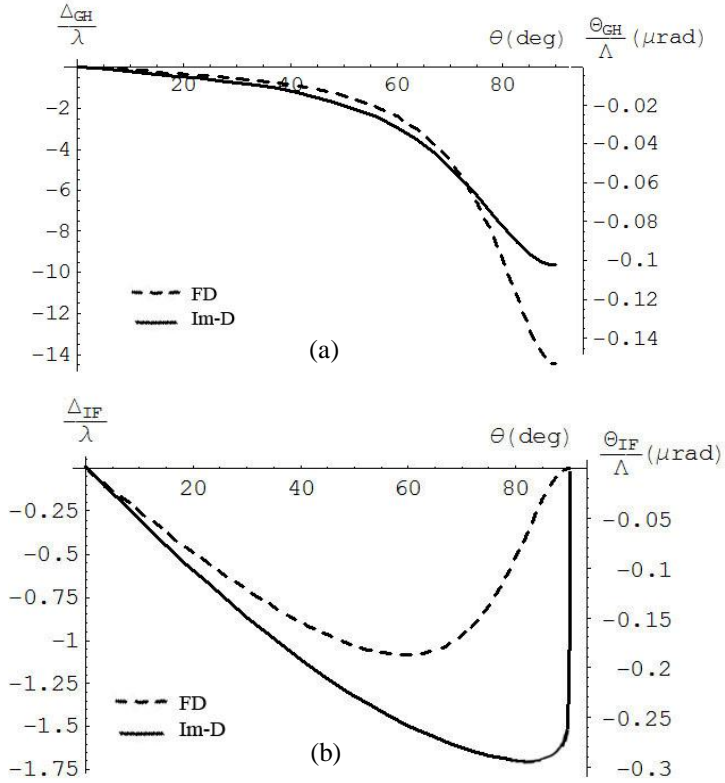
Fig.3. Reflection beam shifts obtained from fundamental Drude model (FD) for bulk gold
and improved Drude model (Im-D) for gold nanoparticles: (a) GH shifts, (b) IF
shifts.

Regarding Fig.3 (a), lateral shifts for angles of incidence greater than 70° reduce
significantly in nanoparticles. The out-of-plane shifts in Fig.3 (b) show a growth
in contrast, and the peak of curve moves toward grazing angles. This may be a
result of dipole-dipole interactions that has proved to become important for
observing the optical properties of nanostructures [29]. In all the calculations
follow henceforth, I will utilize the improved model.

A. Polarization effect

Consider a laser beam that passes a tunable linear polarizer. The outcoming light
with an arbitrary state of polarity radiates on the gold nanoparticle-mirror that is
kept at a definite temperature (as shown in Fig.2). Figure 4 demonstrates the
spatial and angular GH and IF shifts as a function of incident angle for a α^o-
linearly polarized light (from $\alpha=0^o$ to $\alpha=90^o$) where the 50nm target nanoparticles
are at room temperature. According to the plots, reflected beam undergoes

different spatial and angular shifts depending on its state of polarization. Both the lateral and transverse shifts are negative, showing a backward flow of energy from the metal surface. The results indicate a considerable negative amounts of Δ_{GH} for p-wave ($\alpha=0°$) at grazing incidence which descends to the smallest value for the s-wave ($\alpha=90°$) monotonically. On the other hand, the negative transverse shifts Δ_{IF} and Θ_{IF} maximize for polarization 45° at grazing incidence while both p and s-waves cause trivial deviations. It is seen that out-of-plane shifts acquire almost equality of values for complementary polarization states.
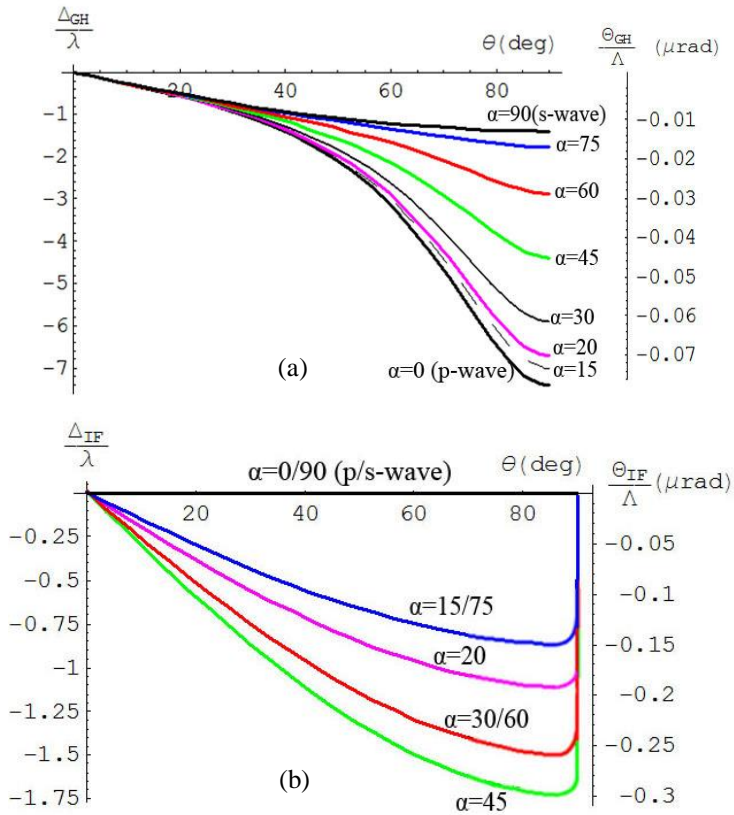

Fig.4 Spatial and angular shifts for different $\alpha°$-linearly polarized beam reflected from a mirror of 50 nm gold nanoparticles at T=300K; (a) Goos-Hanchen shifts, (b) Imbert-Fedorov shifts.

To clarify the influence of particle size, GH and IF shifts are calculated for different radius of nanosphere at a fixed temperature. Figure 5 shows the shifts versus light angle of incidence where the state of polarization is chosen hereafter

to give the maximum shift, i.e. p-wave and 45° polarized for GH and IF deviations respectively. Laser beam radiates on mirror grazingly (see Fig.4).
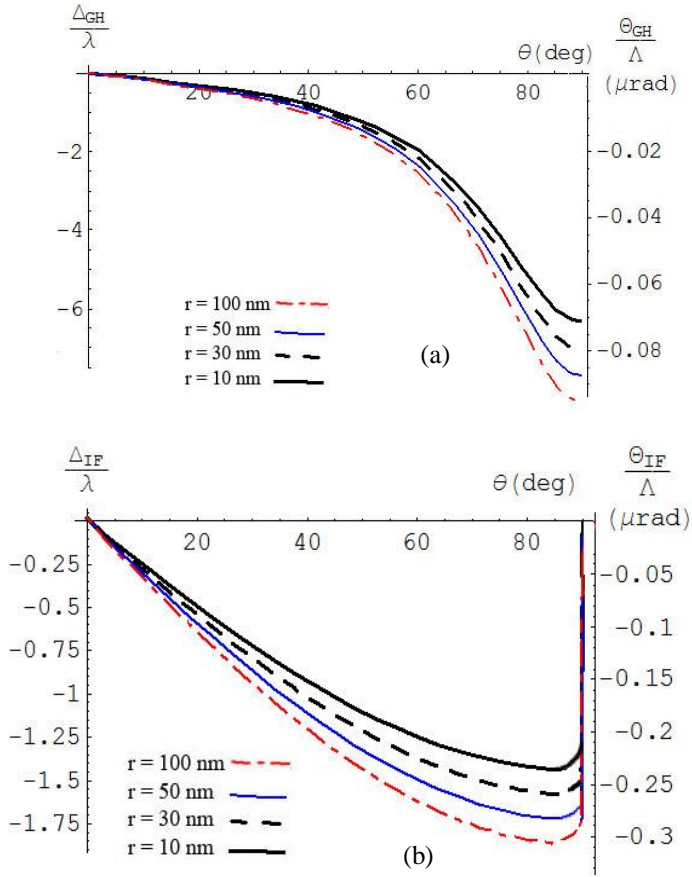

Fig.5 Spatial and angular shifts versus angle of incidence reflected from gold nanoparticles with different sizes at T=300K; (a) Goos-Hanchen shifts, (b) Imbert-Fedorov shifts.

B. Temperature effect

In Fig.6 spatial and angular GH and IF shifts are plotted versus temperature for various nanoparticle radii. It is of interest to note that, the behavior of angular IF shift distinguishes the others: While the GH and spatial IF shifts decline by heating the metal, the angular deviation Θ_{IF} displays an enhancement.
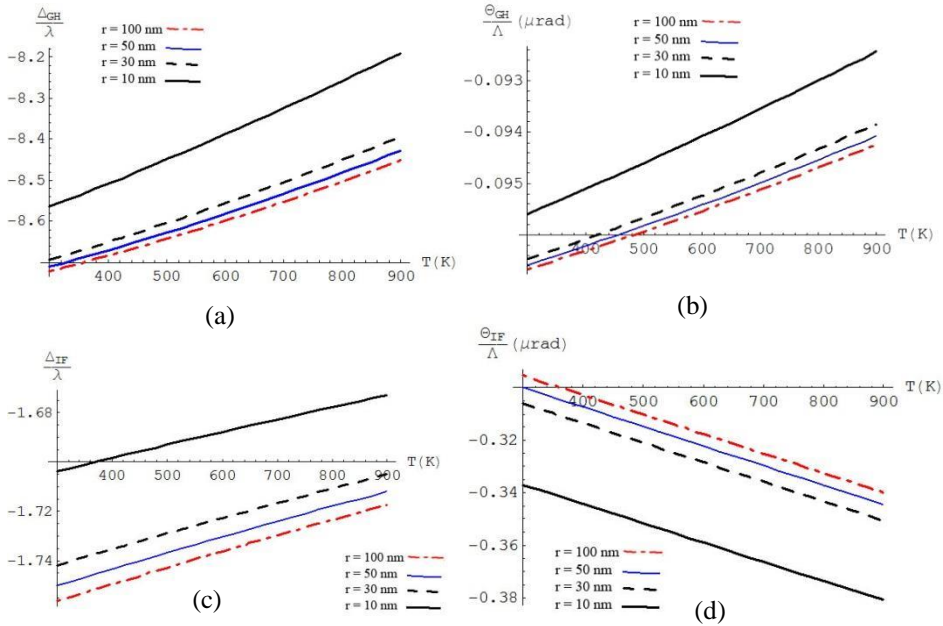
Fig.6 Spatial shifts for p-wave and 45°-linearly polarized He-Ne laser beam reflected from gold nanoparticles as a function of temperature: (a),(b)Goos-Hanchen (c),(d)Imbert-Fedorov.

By the temperature increment, the volume of the nanoparticles increases and the density of the free electrons is reduced. The lower electron density leads to the lower plasma frequency of the electrons. Moreover, the rate of electron–phonon scattering increases with increasing temperature. This leads to the increase of the damping constant of the plasma oscillations and subsequently to the red shift of the SP resonance. The dielectric function of nanoparticles $\varepsilon_{imp}(\omega)$, changes accordingly (see eq. (5)).Enlargement of real part and reduction of imaginary part (R and φ respectively) affects shift deflections in eqs. (2), causing the trends shown in Fig. 6. Due to the eqs.(1) and (2), R_s is impressed more than R_p in this process which justifies the different behavior of Θ_{IF}.

C. Particle size effect

In order to discuss how the particle size affects the shifts, the spatial and angular shifts are now depicted versus radius of nanoparticle at various temperatures in Fig.7. According to the results, the distinct response of Θ_{IF} is repeated for the change in particle size as well; While larger nanospheres in the mirror cause

greater GH shifts (both in spatial and angular portions), the IF counterparts behave oppositely: In another word, Δ_{IF} strengthens and Θ_{IF} decreases.
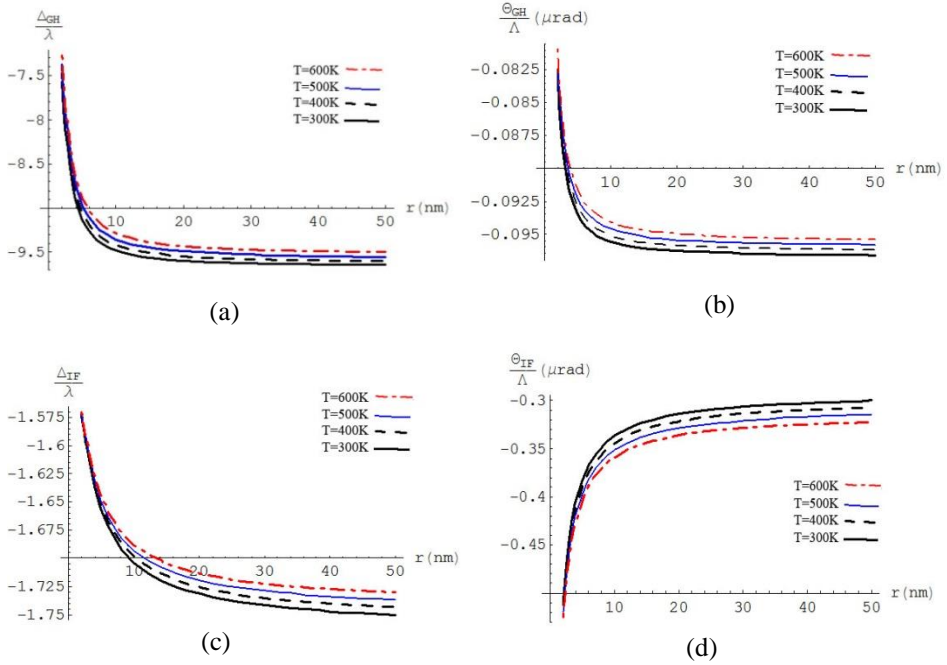

Fig.7 Size dependence of spatial and angular shifts for a linearly polarized He-Ne laser beam reflected from gold nanoparticles at different temperatures: (a),(b) Goos-Hanchen (c),(d)Imbert-Fedorov.

Due to the polarization induced by the incident electric field, each NP assumed to behave like an induced dipole that experiences bonding-type interaction with its neighboring NPs. This interaction strengthens with increasing size of NPs and results in enhancement of reflectance [10]. There is interplay between the effects of simultaneous increase in size of the NPs and their inter-particle coupling. In small radii, reduction of size dependent scattering term (eq. (7)) is dominant. But beyond size of 20nm, the effect of increase in particle interaction starts counteracting scattering effect and hence, the reflection shifts tend to saturate.

3. CONCLUSION

In summary, this work presented a simple improved Drude model to investigate the reflection shifts from a mirror consisting of a monolayer of gold

nanoparticles. Detailed theoretical analysis revealed that oblique polarized light impinging on the mirror could undergo both GH as well as IF shift depending its state of polarity. Both the lateral and transverse shifts are negative, showing a backward flow of energy from the metal surface. The negative transverse shifts Δ_{IF} and Θ_{IF} have a peak for polarization 45° at grazing incidence. These out-of-plane shifts also enjoy an interesting equality of values for complementary polarization angles.

Reflection shifts obviously depend on temperature and nanoparticles' size. Exploration emphasizes that if the mirror's temperature goes up, the amount of all shifts will reduce linearly except in Θ_{IF}. The results also show that temperature spectra of shifts can be adjusted by particle size. Distinct feature of Θ_{IF} recurs for gold nanospheres with various radii. Indeed a monolayer of large nanospheres makes a less angular IF shift compared to those of smaller nanoparticles. A precise control of these deviations can be used as a novel method to determine the size or temperature of gold nanoparticles in a sample. Moreover, the results may prove to be valuable for developing ultra-sensitive sensors in nano-photonics.

REFERENCES

[1] F. Tam and N. Halas. *NPlasmon response of nanoshell dopants in organic films: a simulation study*. Prog Org Coat. 47 (2003) 275–278. Available: nathan.instras .com/ResearchProposalDB/doc-102.pdf

[2] F. Tam, C. Moran and N. Halas. *Geometrical parameters controlling sensitivity of nanoshell plasmon resonances to changes in dielectric environment*. J Phys Chem B. 108, (2004) 17290–17294. Available: http:// pubs. acs. org/ doi/ abs /10.1021 /jp048499x.

[3] D. O'Neal, L. Hirsch et al. *Photothermal tumor ablation in mice using near infrared-absorbing nanoparticles*. Cancer Lett. 209 (2004) 171–176. Available: https://www.ncbi.nlm.nih.gov/pubmed/15159019

[4] K. R. Catchpole, A. Polman. *Design principles for particle plasmon enhanced solar cells*. Appl. Phys. Lett. 93 (2008) 191113. Available: http:// aip. scitation. org/ doi/ abs/10.1063/1.3021072

[5] Ping-Ping Fang et al. *Conductive Gold Nanoparticle Mirrors at Liquid/Liquid Interfaces*. ACS Nano. 7 (10) (2013) 9241–9248. Available: http://pubs.acs. org/ doi/abs/10.1021/nn403879g; S.K. Ghosh, T. Pal. Chem. Rev. 107, (2007) 4797-4862.

[6] L. Fontana et al. *Gold and silver nanoparticles based networks as advanced materials for optoelectronic devices*. Presented at 18th Italian National Conference on Photonic Technologies (Fotonica 2016). Available: http:// ieeexplore. ieee.org/ document/7858049/?reload=true

[7] Y. Shoji, K. Kintaka et al. *Low-crosstalk 2 × 2 thermo optic switch with silicon wire waveguides*. Opt. Express. 18(9) (2010) 9071–9075. Available: https://www.osapublishing.org/abstract.cfm?uri=oe-18-9-9071

[8] M. I. Lapsley, S. S. Lin et al. *An in-plane, variable optical attenuator using a fluid-based tunable reflective interface*. Appl. Phys. Lett. 95(8) (2009) 083507. Available: http://aip.scitation.org/doi/abs/10.1063/1.3213348

[9] T. Ochiai et al. *Enhancement of self-assembly of large (>10 nm) gold nanoparticles on an ITO substrate*. Appl. Phys. Express 7 (2014) 065001. Available: http://iopscience.iop.org/article/10.7567/APEX.7.065001/pdf

[10] D. Wan et al. *Using Spectroscopic Ellipsometry to Characterize and Apply the Optical Constants of Hollow Gold Nanoparticles*. ACS nano. 3 (4) (2009) 960-970. Available: http://pubs.acs.org/doi/abs/10.1021/nn8009008

[11] G. Jayaswal, G. Mistura and M. Merano. *Weak measurement of the Goos-Hanchen shift*. Opt. Lett. 38, 1232–1234(2013). Available: https:// www. osapublishing.org/abstract.cfm?uri=ol-38-8-1232

[12] W. Löffler et al. *Polarization-dependent Goos–Hänchen shift at a graded dielectric interface*. Opt. Commun. 283, 18, (2010) 3367–3370. Available:

[13] H. M. Lai, S.W. Chan et al. *Nonspecular effects on reflection from absorbing media at and around Brewster's dip*. J. Opt. Soc. Am., 23 (2006) 3208. Available: https://www.ncbi.nlm.nih.gov/pubmed/17106478

[14] L. G. Wang et al. *Negative and Positive Lateral Shift of a Light Beam Reflected from a Grounded slab*. Opt. Lett. 31(8) (2006) 1124-1126. Available: https://pdfs.semanticscholar.org/33c4/83981f7d39d151f6ba9022702a66ecdc9cac.pdf

[15] S. Grosche, M. Ornigotti et al. *Goos-Hänchen and Imbert-Fedorov shifts for Gaussian beams impinging on graphene-coated surfaces*. Opt. Express. 16 (2015) 23. Available: https://www.osapublishing.org/abstract.cfm?uri=oe-23-23-30195

[16] V. J. Yallapragada, A. P. Ravishankar et al. *Observation of giant Goos-Hänchen and angular shifts at designed metasurfaces*. Scientific Reports. 6 (2016) 19319. Available: https://www.nature.com/articles/srep19319

[17] Y. Wan , Z. Zheng, W. Kong et al., *Fiber-to-fiber optical switching based on gigantic Bloch-surface-wave-induced Goos-Hänchen shifts*. J. Photon. 5 (2013) 7200107. Available: http:// ieeexplore. ieee.org/ iel5/ 4563994/ 6428647/ 06384639.pdf

[18] X. Wang, M. Sang et al., IEEE Photonics Technology Lett. 28 (3) (2015).

[19] M. Born and E. Wolf, *Principles of Optics*, 7th ed., Pergamon Press, London, 2005.

[20] F. Goos and H. Hanchen. *Ein neuer und fundamentaler Versuch zur Total reflexion.* Ann. Phys. 436 (1947) 333–346. Available: onlinelibrary. wiley. com/doi/10.1002/andp.19474360704/abstract

[21] C. Imbert. *Calculation and Experimental Proof of the Transverse Shift Induced by Total Internal Reflection of a Circularly Polarized Light Beam.* Phys. Rev. D. 5 (1972) 787. Available: https://journals.aps.org/prd/abstract/10.1103/PhysRevD.5.787

[22] F.I. Fedorov et al. *On the theory of total internal reflection.* SSSR. 105 (3) (1955) 465-468.

[23] A. Y. Qin, Y. Li et al. *Measurement of spin Hall effect of reflected light.* Opt. Lett. 34, (2009)2551–2553. Available: https:// www. osapublishing. org/ abstract. cfm?uri=ol-34-17-2551; V. Fedoseyev. *Conservation laws and angular transverse shifts of the reflected and transmitted light beams*. Opt. Commun. 282 (2009)1247–1251. Available: https:// www. sciencedirect. com/ science/article/pii/S0030401808012571

[24] H. M. Lai, C. W. Kwok et al. *Energy-flux pattern in the Goos-Hänchen effect.* Phys. Rev. E. 62 (2000) 7330. Available: https:// www. researchgate. net/.../12226103_Energy-flux_pattern_in_the_Goos-Hanchen effect

[25] M. Ornigotti and A. Aiello. *Goos–Hänchen and Imbert–Fedorov shifts for bounded wavepackets of light.* J. Opt. 15 (2013) 014004. Available: http://iopscience.iop.org/article/10.1088/2040-8978/15/1/014004/meta

[26] R. Tsekov et al. *Quantifying the Blue Shift in the Light Absorption of Small Gold Nanoparticles.* Available: https://arxiv.org/pdf/1702.04513

[27] O. A. Yeshchenko. *Temperature effects on the surface plasmon resonance in copper nanoparticles.* Ukrainian Journal of Physics. 3 (58) (2013) 249-259. Available: https://arxiv.org/abs/1303.3778

[28] Lucia B Scaffardi and Jorge O Tocho. *Size dependence of refractive index of gold Nanoparticles.* Nanotechnology, 17 (2006) 1309–1315. Available: http://iopscience.iop.org/article/10.1088/0957-4484/17/5/024/meta

[29] G. Solookinejad, M. Panahi et al. *Giant Goos-Hänchen Shifts in Polaritonic Materials Doped with Nanoparticles.* Plasmonics 12(3) (2017) 849-854. Available:https://www.sparrho.com/item/giant-goos-hanchen-shifts-in-polaritonic materials-doped-with-nanoparticles/a61134/